Leakage and Impact Detection of Subsea Pipelines using Fiber Bragg Grating Sensors

A Thesis

Presented to

The Faculty of the Department of Mechanical Engineering

University of Houston

In Partial Fulfillment

Of the Requirement for the Degree

Master of Science

In Mechanical Engineering

By

Saeid Amiri

December 2015

Leakage and Impact Detection of Subsea Pipelines using Fiber Bragg Grating Sensors

Saeid Amiri

Approved:

Chair of the Committee
Gangbing Song, Professor,
Mechanical Engineering

Committee Members:

Jae-Hyun Ryou, Assistant Professor
Mechanical Engineering

Gino J. Lim, Associate Professor
Industrial Engineering

Siu Chun Michael Ho, Research Associate
Mechanical Engineering

Suresh K. Khator, Associate Dean,
Cullen College of Engineering

Pradeep Sharma, Professor and Chair,
Mechanical Engineering

Acknowledgment

Firstly, I would like to express my sincere gratitude to my advisor, Professor Song for the continuous support of my Masters study, for his patience, motivation, and immense knowledge. His guidance helped me in all the time of research and writing of this thesis. I could not have imagined having a better advisor and mentor for my thesis.

My co-advisor, Dr. Michael Ho, has been always there to listen and give advice. I am deeply grateful to him for the discussions that helped me sort out the technical details of my work. I am also thankful to him for encouraging the use of correct grammar and consistent notation in my writings and for carefully reading and commenting on countless revisions of my thesis.

In the committee I would like thank Professors Lim and Ryou for their responses to all my emails (late and early) and for accepting to be in my thesis committee.

To my family, I thank my parents and brothers for supporting me emotionally and mentally when I got stuck or needed reclusion.

I also acknowledge National Science foundation (NSF) and OneSubsea LLC for their support for this project.

Without the support, encouragement, and dedication to assist me, this dissertation would not have been possible.

Leakage and Impact Detection of Subsea Pipelines using Fiber Bragg Grating Sensors

An Abstract

of a

A thesis

Presented to

The Faculty of the Department of Mechanical Engineering

University of Houston

In Partial Fulfillment

Of the Requirements for the Degree

Master of Science

In Mechanical Engineering

By

Saeid Amiri

December 2015

Abstract

In this thesis, a novel method is proposed to calculate the leakage and impact location of the pipelines using Fiber Bragg Grating (FBG) sensors. Detection for leakage was accomplished through the measurement of the negative pressure wave (NPW) resulted from rapid depressurization of a gas pipeline. Experiments were performed on a model PVC pipeline (180 ft) with five manually controlled leakage points. Leakage was detected with 6-20% error, with higher error skewed towards the ends of the pipeline due to reflective boundary conditions. Meanwhile, impact experiment were also conducted on the pipeline. Impact was detected and impact points were localized using a similar algorithm. However, impact-induced stress waves were used instead of NPW. Similar to leakage detection, accuracy was affected by pipeline length and also sampling frequency. Results in this thesis set the foundation for future fiber-optic based pipeline monitoring systems that may prevent and mitigate damage caused by pipeline failures.

Table of Contents

Contents

List of Figures

List of Tables

Nomenclature

Term	Definition
ABC	Artificial Bee Colony
EMI	Electromagnetic interference
EPI	Electric Power Industry
FBG	Fiber Bragg Grating
FEM	Finite Element Modeling
FRD	Frequency Response Diagram
FWHM	Full Width Half maximum
LPV	Linear Parameter Varying
NDE	Non Destructive Examination
NPW	Negative pressure Wave
FOS	Fiber Optical Sensors
SHM	Structural Health Monitoring
SVM	Support Vector Machine
WDM	Wavelength Division Multiplexing

1. Introduction

Pipelines are one of the largest infrastructures in Oil and Gas industry. Therefore, it is quite vital to have constant monitoring on them because of the integrity concerns. It will yield the reduction of maintenance costs and prevent hazardous consequences. Some possible incidents that might happen to pipelines are leakage, third party intrusion, flow assurance issues such as wax and hydrate formation, deformation due to buckling and soil settlement.

In the current thesis, two possible incidents, leakage and impact on pipelines are studied by conducting experiments on PVC pipes and using Fiber Bragg Grating sensors, one specific type of fiber optic sensors.

1.1. Structural Health Monitoring of Pipelines

Pipeline monitoring presents unique challenges. Their long length, high value, high risk and often difficult access conditions require continuous monitoring and optimization of maintenance. Structural health monitoring can be classified into five levels in terms of complexity [1] as listed in Table 1:

Table 1- Levels of structural health monitoring

Level number	Definition
Level 1	Detect Presence of Damage
Level 2	Level 1 and Location of Damage
Level 3	Level 2 and Severity of Damage: Diagnosis
Level 4	Level 3 and Consequences of damage: Prognosis
Level 5	Level 4 and Self-diagnosis, Self-prognosis, Self-healing

In level 1, SHM only detects the presence of the damage without localizing it. In level 2, SHM is capable of finding the location of the damage as well, which is the level that current thesis has achieved. In level 3, SHM can find how severe the damage is by measuring the intensity of the impact force or finding how big or small the damage is. In level 4, SHM systems are able to carry out the prognosis or to estimate the remaining service life. Finally, in level 5, SHM covers all the previous levels as well as doing self-diagnosis, self-prognosis and self-healing.

Structural health monitoring consists of 24/7 continuous recording of key structural and environmental parameters. The information obtained from monitoring is generally used to plan and design maintenance activities, increase the safety, reduce maintenance costs and widening the knowledge concerning the structure being monitored [2]. Thus, safety is increased, maintenance cost is optimized and economic losses are decreased. Many infrastructures, such as bridges and dams are at their design life but they can remain in service if there is proper monitoring.

Fiber optic sensors are among the relative brand-new sensors in science and technology. Their wide range of applications and considerable advantages have been the major driver for researchers to study on them. They are able to measure parameters such as temperature, strain, load and pressure along a single fiber, which is a good choice for monitoring of gigantic structures such as flowlines and bridges [3]. Although some telecommunications cables can be effectively used for sensing ordinary temperatures, monitoring high and low temperatures or distributed strain presents unique challenges that require specific cable designs [4].

Flowlines usually are embedded in dangerous areas and they are prone to natural incidents such as landslides, earthquakes or they can be influenced by third party such as obstruction, hot tapping, vandalism or trawling for subsea pipelines. Any of such incidents can have a major change in the flowline health leading to damage, leakage and failure with serious economic and ecological consequences. In addition, wear can be induced by the operational conditions. By constant monitoring of temperature, pressure and strain changes possible incidents can be prevented [5].

Since flowlines typically are so long it is impossible to use many discrete sensors. Also installation of them requires a large number of cables and data acquisition system which results in increase of the costs. Other current monitoring methods include flow measurements at the beginning and the end of the pipeline, offering an indication of the presence of a leak, but little information on its location [6]. One of the major possible incidents for pipelines is leakage that is caused by many factors that could be

deformation induced by earthquakes, landslide or collisions made by ship anchors, corrosion or material defect [7].

Furthermore, it is often possible to detect damage even before a critical state is reached. This is possible by using fiber optic sensors and measuring the strain along the pipeline [8]. Also, temperature and strain monitoring can detect third party intrusion before any damage is done to the pipeline.

1.2. Fiber Optic Sensing

Optical fibers can be used in a variety of applications including telecommunication as well as sensing purposes. Fiber optic sensors are small enough to fit in confined areas and can be positioned precisely where needed with flexible fibers.

1.2.1. Background

Fiber optic sensors have a wide range of applications. They can be used to measure many parameters such as strain, vibration of structures and machines, electric current, voltage, impedance, leakage current of insulators, temperature, pressure and gas concentration [9].

In the electrical power industry (EPI), there are two common problems that can cause failure of an electronic sensor: high voltage and high electromagnetic interference (EMI) [11]. Therefore, depending on the place of the measurement of a parameter, it can be very difficult or even impossible to use a conventional sensor. The best option to prevent this problem is using FOS. Since the fiber is made of dielectric material glass, it is

possible to place them very close to a high potential conductor. As the sensor is optical based, the sensor does not need electrical power delivered to its location.

Another problem with conventional sensors is that they all need electric energy to work. However, providing electric energy at the sensor location is sometimes difficult if the device needs to be far away from any appropriated power supply or if the structure is in contact with water.

FOS does not require electric energy to work. Therefore some very specific characteristics of FOS are high immunity to EMI, electrical insulation, absence of metallic parts, not requiring local electrical power, lightweight and compactness, easy maintenance, chemically inert even against corrosion, work over long distances and several sensors can be multiplexed on the same fiber [10].

All fiber optic sensors can be classified into four different types in terms of sensing principle [1] and a comparison of all types of FOS sensors are in Table 2 [2] :

1) **Local**: When the measurement is carried out at discrete points accessed by different channels. In other words, each sensor detects at only one point.

2) **Quasi-distributed**: FBG sensors are the most common type of such sensors. They are capable of measuring the variable value at discrete points in a single span of optical fiber.

3) **Distributed**: They can measure the value of the measurand along a line of space with a given resolution in a continuous way at each point of space.

Table 2-Different types of FOS sensors

Type	Mesurand	Linear Response	Resolution	Modulation method
Local	Strain	Y	0.01% gage length	Phase
	Displacement	Y	0.2% gage length	Phase
Quasi-distributed	Strain	Y	1 μ strain	Wavelength
Distributed	Temperature /Strain	N	0.5 m/C	Intensity
	Temperature /Strain	N	0.5 m/C	Intensity

1.2.2. Theory and Models of FBG

Fiber Bragg Grating (FBG) technology is one of the most popular choices for optical fiber sensors for strain or temperature measurements due to their reliability and commercial availability. They are made by periodic inscription of UV laser which creates periodic gratings along the fiber. As a result, a periodic change in the refractive index is created [11].

After the inscription of the grating into the fiber's core, due to the periodic modulation of the index of refraction, light guided along the core of the fiber will be weakly reflected by each grating plane [9]. The reflected light from each grating plane

will join together with the other reflections in the backward direction. The distances traveled by light are affected by the index of refraction of the fiber in eqn. (1) [11]:

$$\lambda_B=2n_{eff}\Lambda. \quad (1)$$

Therefore the Bragg wavelength (λ_B) of an FBG is a function of the effective refractive index of the fiber (n_{eff}) and the periodicity of the grating (Λ). In eqn. (2), λ_B is the peak wavelength of the narrowband spectral component reflected by the FBG. The FWHM (full width-half maximum) or bandwidth of this reflection depends on several parameters, particularly the grating length. Typically, the FWHM is 0.05 to 0.3 nm in most sensor applications. Figure 1 shows a typical Bragg reflection peak [9]. From eqn. (1), it can be seen that the Bragg wavelength only depends on the distance between gratings (Λ) and the effective index of refraction (n_{eff}).

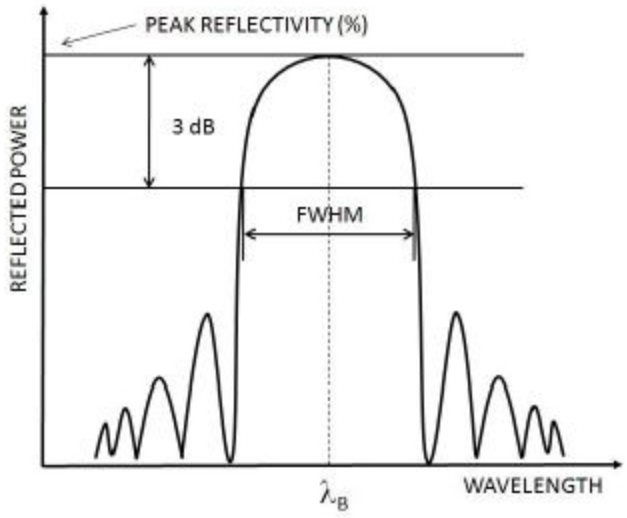

Figure 1-A typical Bragg reflection wave shape with its parameters defined [9]

FBG is essentially a sensor of temperature and strain. However by designing the proper interface, many other measurements can be made to impose perturbation on the grating resulting in a shift in the Bragg wavelength which can then be used as a parameter transducer. Therefore, by using an FBG as a sensor, one can obtain measurements of strain, temperature, pressure, vibration and displacement.

Changes in strain and temperature affect the effective refractive index and the grating period (Λ) of an FBG, which results in a change in the reflected Bragg wavelength (λ_B) according to eqn. (1). Thus, the wavelength change can be measured to determine the corresponding change in strain and temperature. Because both strain and temperature affect the Bragg wavelength, temperature compensation is an important consideration for large temperature or strain range tests. At each periodic refraction change, a small amount of light is reflected.

When the broad band light which covers a spectrum of various wavelengths travels along the fiber, as it reaches the periodic gratings, because of the change in the refractive index a portion of the spectrum with a specific wavelength is reflected. All the reflected light are in phase and constructively interfere at a particular wavelength when the grating period is approximately half the input light's wavelength. Therefore, light propagates through the gratings with negligible attenuation. Only those wavelengths that satisfy the Bragg condition are affected and reflected. This is the main ability and advantage of fiber Bragg gratings.

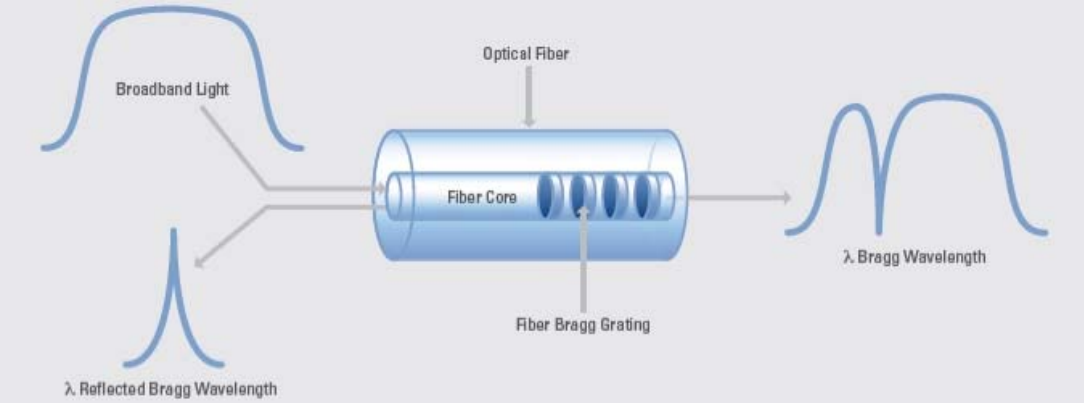

Figure 2-Fiber Bragg Grating mechanism [11]

The ability to write FBGs with unique Bragg wavelengths lends itself well to wavelength division multiplexing (WDM) techniques [15]. This provides the ability of using multiple sensors with different Bragg wavelengths along a single fiber over long distances. WDM provides each FBG sensor a unique wavelength range within the light spectrum. Because of the wavelength nature of FBG, sensor measurements remain accurate even with light intensity losses/attenuations due to bending or transmission. The schematic drawing of the grating periods and the reflected spectrum are shown in Figure 2 .

This spectral component will be missed in the transmitted signal, but the remainder of this light may be used to illuminate other FBGs in the same fiber, with each one tuned to a different Bragg wavelength. The final result of such an arrangement is that we will have all Bragg peak reflections of each FBG back at the beginning of the fiber, each one in its specific wavelength range. The relation between the wavelength variation, strain and temperature is given by eqn. 2 as

$$\frac{\Delta\lambda_B}{\lambda_B}=\left(1-\rho_e\right)\varepsilon_z+(\alpha+\eta)\Delta T, \quad (2)$$

Where λ_B is the Bragg wavelength, ρ_e is the photo-elastic coefficient, ε_z the longitudal strain, α is the thermal expansion, η is the thermo-optic coefficient, ΔT is the temperature variation. The coefficient values for a silica fiber with a germanium doped core are as $\rho_e=0.22$, $\alpha=0.55\times10^{-6}\frac{1}{C}$ and $\eta=0.55\times10^{-6}\frac{1}{C}$.

2. Leakage Detection

The generation of leak along the pipeline carrying crude oils and liquid fuels results enormous financial loss to the industry and also affects the public health. Hence, the leak detection and localization problem have always been a major concern for the companies. In spite of the various techniques developed, accuracy and time involved in the prediction is still a matter of concern.

2.1. Literature

Kim [11] analyzed the oscillatory flows in pipeline systems due to excitation by valve operation using impulse response method. He integrated the genetic algorithm into the impulse response method to calibrate the location and the quantity of leakage. Hou et al. [12] found the pipeline leakage based on the negative pressure wave with a slight deformation to the diameter of pipeline using FBG sensors. Huang et al. [13] designed an FBG pressure sensor and implemented to detect the leakage of prestressed concrete cylinder pipe with two FBGs bonded on its outside and inside surfaces. Ma et al. [14] designed a new method to solve the problem of high false alarm rate and low positioning accuracy in the gas leak location detection. They used negative pressure wave signal combined with flow balance.

Mandal et al. [15] proposed a novel leak detection scheme based on rough set theory and support vector machine (SVM) to overcome the problem of false leak detection. Further, they employed SVM classifier to inspect the cases that could not be

detected by applied rules. For the computational training of SVM, they used swarm intelligence technique: artificial bee colony (ABC) algorithm. Da Silva [16] presented a methodology for pipeline leakage detection using a combination of clustering and classification tools for fault detection. They used a fuzzy system to classify the running mode and identify the operational and process transients. The results were very encouraging with relatively low levels of false alarms. Qiong and Shidong [17] developed a pipeline leak detection system based on virtual instrument LabVIEW and described the system principle, composition structure and development progress in detail. The pipeline leak detection system acquired pressure and flow at two ends of the pipeline in real time, analyzed data by wavelet analysis functions offered by LabVIEW, detected leak through flow changes and located leak by negative pressure wave method. Laurentys et al. [18] proposed a set of models acting as expert systems: each one observing and diagnosing pipeline leakage in real-time. A set of techniques they applied in order to be possible for the system to execute its function consists of fuzzy logic, neural network, genetic algorithm and statistical analysis. Lu et al. [19] brought forward constitution of pipeline leakage detection system, introduced the main method of the leakage detection and then gave a detailed explanation of the properties of wavelet transform and de-noising principle. Hou et al. [20] proposed an improved negative pressure wave method based on FBG based strain sensors and wavelet analysis using FBG based sensors. Verde [21] proposed an approach to detect leak locations in a pipeline using only sensors of flow and pressure at the ends of the duct, assuming a simple nonlinear model of the fluid

in a pipeline with leaks, discretizing the special variable in nonuniform sections with unknown boundaries that depend on the leaks locations. Lee et al. [22] presented a method for leak detection in single pipe where the behavior of the system frequency response diagram (FRD) was used as an indicator of the pipe integrity. The presence of a leak in a pipe imposes a pattern on the resonance peaks of the FRD that can be used as a clear indication of leakage. Dos Santos et al. [23] proposed a new approach to gas leakage detection in high pressure distribution networks, where two leakage detectors were modelled as a linear parameter varying (LPV). Each leakage detector uses two Kalman filters and the fault is viewed as an augmented state.

2.2. Methodology

The method to find the leakage location is based on negative pressure wave (NPW). When the pipeline leaks, the internal pressure at leak point decreases rapidly due to the loss of pipe contents. The pressure drop propagates along the pipe as a wave towards the pipe ends. The signal of pressure reduction is collected by sensors installed on both ends of the pipeline. Based on the time difference that pressure sensors on both ends detect, pipe length and NPW velocity (285 m/s), the leak point can be estimated [24].

Also, the internal pressure change of the pipe is proportional to the pipe circumferential strain based on eqn. (3):

$$\varepsilon = \frac{\sigma}{E} = \frac{PR}{Et}, \tag{3}$$

where ε is pipe wall circumferential strain, σ is pipe wall hoop stress, E is pipe elastic modulus, t is the pipe wall thickness, R is the pipe radius and P is the internal pressure of the pipe. Based on eqn. (3), when the pipe pressure changes, the pipe circumferential strain also changes. Therefore, when the pipeline leaks somewhere, there will be an instantaneous pressure drop as a pressure reducing wave source spread through the pipeline.

As the NPW propagates along the pipeline, many factors affect its attenuation. Ge et al. [25] has derived the attenuation equation of the pressure wave in eqn. (4):

$$\left|P_{L_p}\right| = |\Delta P| \left|1 - \frac{A}{a} R\left(L_p - 1\right)\right| \text{ and} \tag{4.1}$$

$$= \left| \frac{C_k^2 A_k^2 \rho a^2 - C_k A_k a \sqrt{\rho(8A^2 P_l + C_k^2 A_k^2 \rho a^2)}}{4A^2} + P_g \right| \left| 1 - \frac{f\bar{Q}}{aA_p D}(L_p - 1) \right|, \tag{4.2}$$

where L_p denotes the length of the pipeline, C_k the discharge coefficient, A_k the area of the leakage orifice, a is the NPW speed, P_g denotes the pressure relative to the barometric pressure around the outside wall and ρ is the fluid density. Also, the velocity of the wave propagation can be found in eqn. (5):

$$V_w = \sqrt{\frac{k/\rho}{1 + \frac{kD}{Ee} C_1}}, \tag{5}$$

where k is the gas volume elasticity coefficient, ρ is the gas density, D is the pipe diameter, e is the pipe wall thickness, E is the elastic Young modulus and C_1 is the pipe restraint coefficient.

2.3. Experimental Setup

The main experiment components were PVC pipes, FBG sensors, interrogator, air pump, ball valves and a laptop for processing the data. More information about each of these components are presented in the following sections. Figure 3 shows the schematic drawing of the pipeline in the experiment with the dimensions. S_1 and S_2 are the two FBG sensors mounted at the beginning and end of the pipeline. L_1, L_2, L_3, L_4 and L_5 are the ball valves used to initiate leakage in the pressured pipeline. Figure 4 shows the experiment set up with all sensors installed on it.

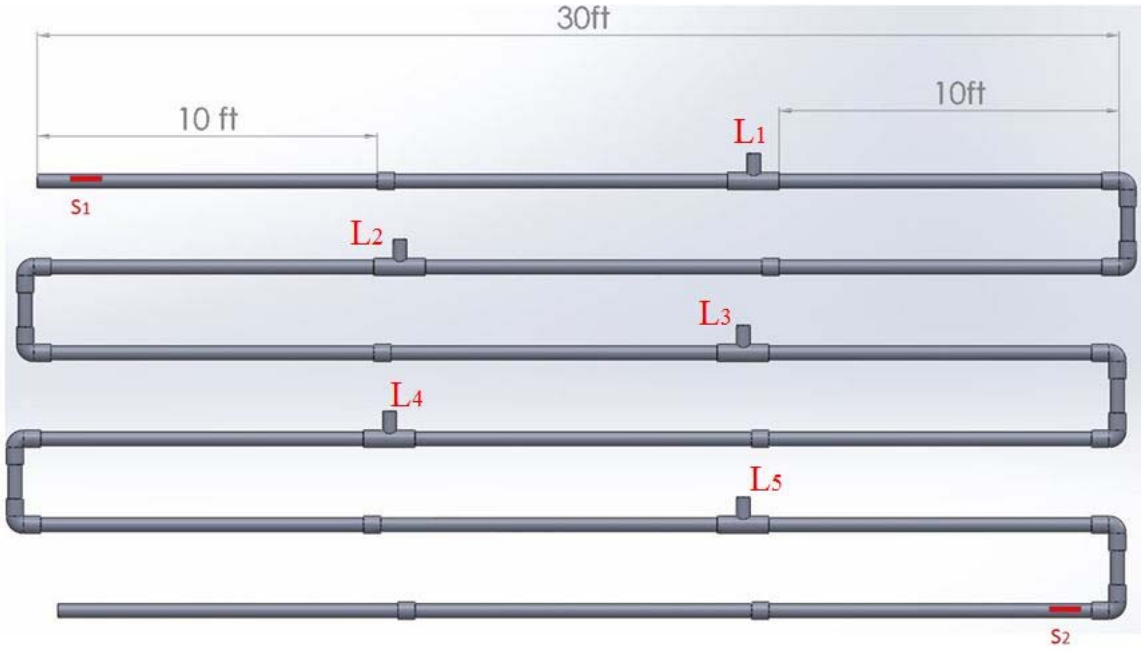

Figure 3-Schematic layout of the experiment

Figure 4- The experimental set up

2.3.1. Pipe

The information about PVC pipe used in the experiment is given in Table 3. The total length of the pipeline is 185 ft.

Table 3- PVC pipeline specifications

Product name	Diameter	Thickness	Material	Density	Young modulus
Schedule 40	1.05 in	0.12 in	PVC	1.45 g/cm^3	1.5 GPa

The pipe path was bended at certain points in order to use an efficient amount of space as shown in Figure 5 . The pipe was divided into six rows, each of 30 ft pipe each assembled together with 90 degrees connectors. The whole setup was clamped on a wooden surface.

Figure 5-The U section of the pipe

Ball valves are durable, performing well after many cycles, and reliable, closing securely even after long periods of disuse. These qualities make them an excellent choice for this experiment as seen in Figure 6.

Figure 6-Ball valves to cause leakage in the pressured pipe

The ball valve's ease of operation, repair, and versatility lend it to extensive industrial use, supporting pressures up to 1000 bar and temperatures up to 752°F (500°C), depending on design and materials used. The best way to measure strain changes in the leakage experiment is to mount and bond the FBG sensor in circumferential direction so that hoop strain is measured more accurately as seen in Figure 7 and Figure 8.

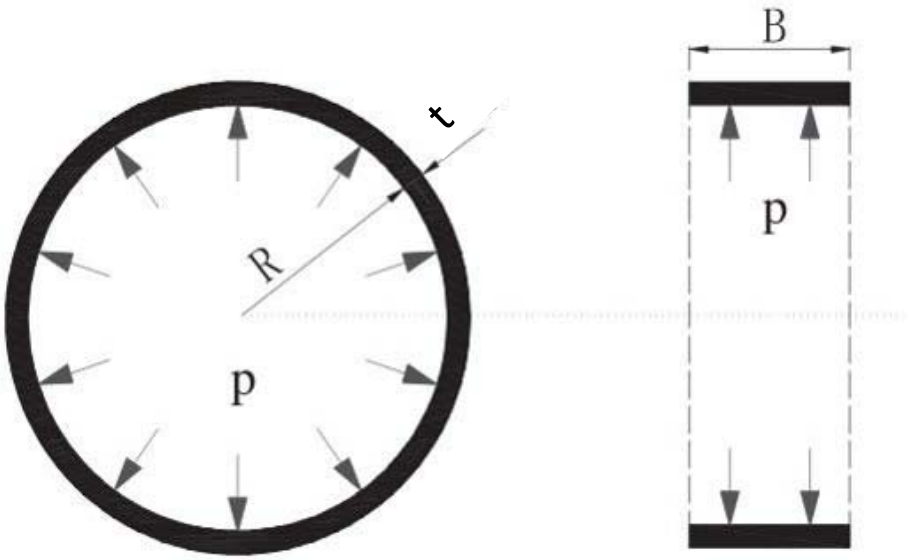

Figure 7-Schematic drawing of sensor orientation [26]

Figure 8-Picture of one installed sensor on the pipe

2.3.2. Data Acquisition

Figure 9-The interrogator-sm130 Field module [27]

The data acquisition device (sm130-700, Micron Optics) used for this experiment is called interrogator which sends light to the sensors and receives the reflected wavelength. The device uses wavelength division multiplexing (WDM) technique which provides the ability to multiplex multiple sensors with different Bragg wavelengths along a single fiber over long distances. Due to the reliance of FBGs on wavelength modulation, sensor measurements remain accurate even with light intensity losses due to bending or transmission. The photo of the interrogator used for the experiment can be seen in Figure 9 and the technical specifications are listed in Table 4.

Table 4- The interrogator specification

Model	Sm130-700
Number of optical channels	4
Scan frequency	1 KHz
Typical FBG sensor capacity	80
Wavelength range	1510-1590 nm
FBG sensor capacity	80

2.3.3. Development of the LabVIEW Code

The LabVIEW code for this experiment conducts the real-time monitoring for detecting the leakage location. The code received the data from each sensor and then converts the wavelength changes into microstrain with the relation in eqn. (6)

$$\frac{\Delta\lambda_B}{\lambda_B}=\left(1-\rho_e\right)\varepsilon, \tag{6}$$

which is the simplified form of eqn. (2). Because in this experiment, the temperature is constant.

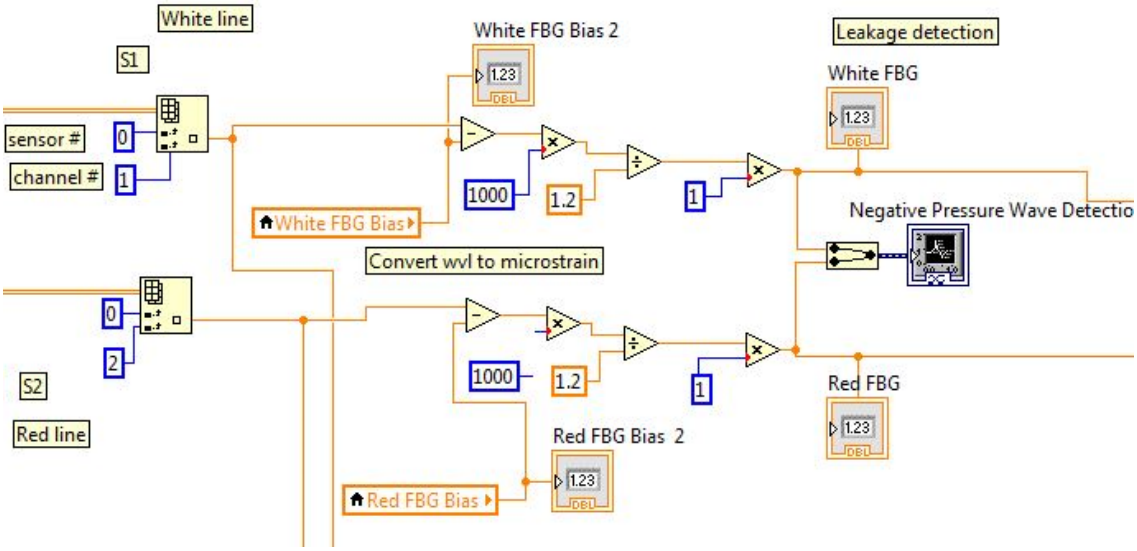

Figure 10-LabVIEW block diagram panel

Figure 10 partially shows the block diagram of the code where the received signal is converted to microstrain. Once one of the valves is opened, there will be a sudden decrease in pressure that results in a sudden decrease in the hoop strain of the pipe affecting the FBG sensor wavelength. In order to find the negative pressure wave time difference, a threshold peak detector is used to find the threshold values and their corresponding times. Once, the arrival time of each sensor is found, with having the velocity of the wave propagation, the location of the leakage is estimated. With the velocity of V=937.5 ft/s=285.75 m/s, the theoretical arrival time differences can be listed as in Table 5.

Table 5- A Time difference to the sensors for leakage experiment

Valve numbers	Distance from S1(ft)	Time travel to S1(s)	Distance from S2(ft)	Time travel to S2(s)	Time difference
L1	15.00	0.0160	136.25	0.1453	-0.1293
L2	45.25	0.0482	106.10	0.1130	-0.0648
L3	75.50	0.0805	75.50	0.0808	-0.0002
L4	105.75	0.1128	45.50	0.0485	0.0642
L5	136.00	0.1450	15.25	0.0162	0.1288

Having the time difference and the velocity known, one can find the location with eqn. (7) given by

$$X=\frac{L+V\Delta T}{2}, \tag{7}$$

and the derivation of this formula is in Appendix 1. Each time a valve is opened, there will be a bias in the values of each sensor. In order to cancel the bias, the operator can reset the experiment which subtracts the wavelength value from the first data. As a result, the average of strain changes of each sensor will be around zero.

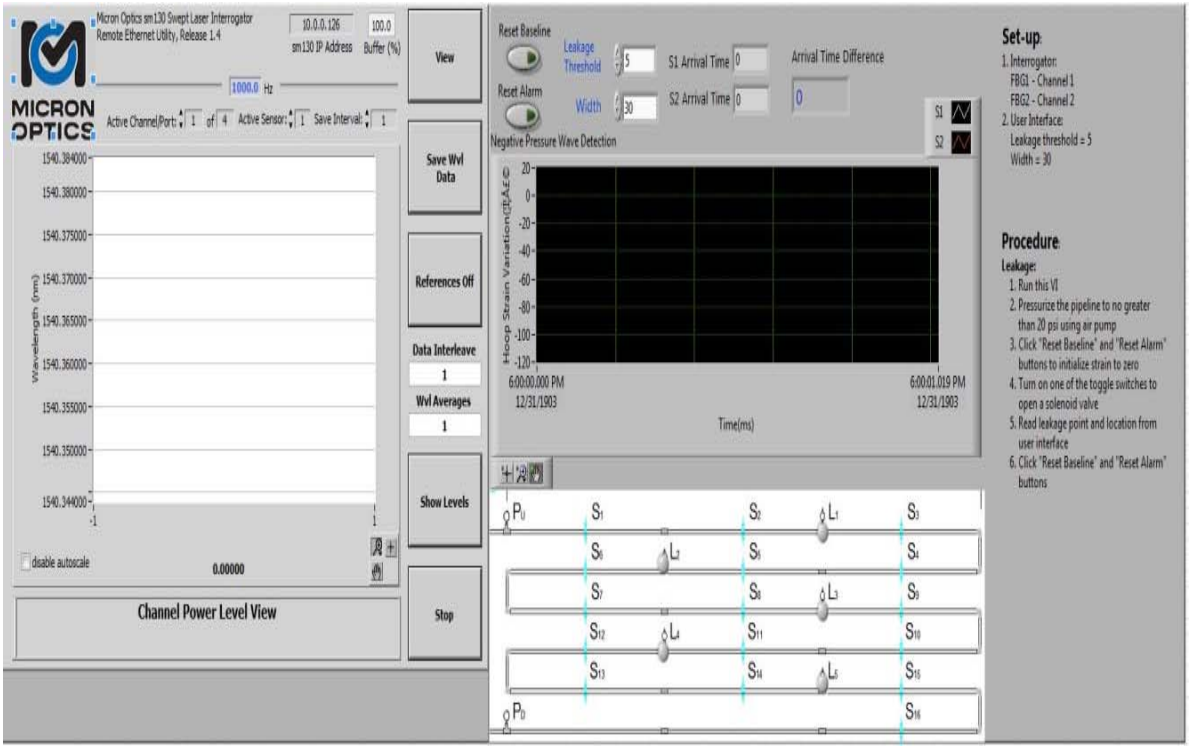

Figure 11-Front panel of the LabVIEW code

Figure 11 shows the front panel of the LabVIEW code where the user can observe the wavelength variations as well as graphical representation of leakage points using Boolean indicators. The graphic interface allows the operator to set the desired threshold value in order not to let the signal noise to be considered in the programming calculations. After each experiment, because of the bias in the wavelengths of each signal, the user has to hit the reset buttons so that the bias is filtered out. Similar real-time plot on the left side of the figure shows the wavelength variations of each sensor versus time.

2.4. Experimental Results

Figure 12 shows the variation in wavelengths of the two FBG sensors in the experiment. The time difference of the two arrived signals is -0.115 s which is closest to the time of valve 1 in Table 3. Due to the reduction of the pressure inside the pipeline as the result of the leakage, the wavelength of the sensor has decreased. The time difference between the two sensors can be seen in this figure.

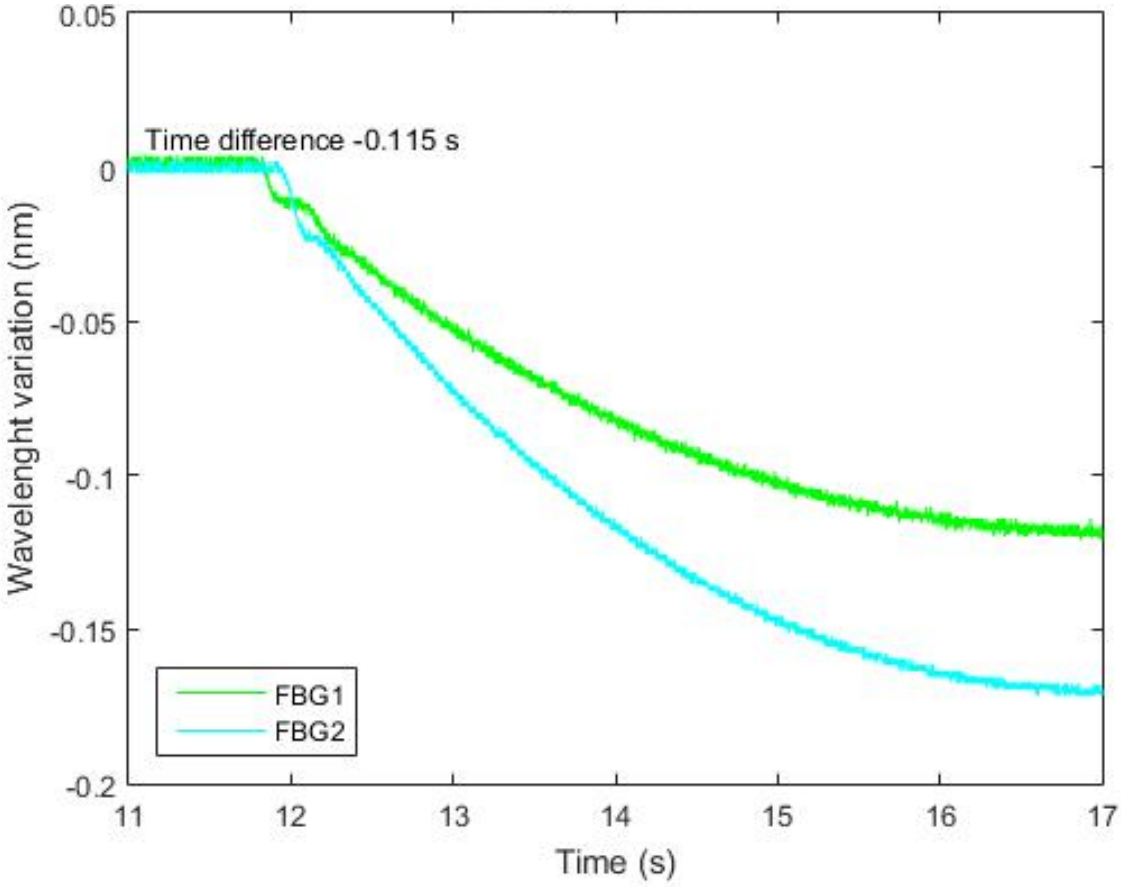

Figure 12-Wavelength decrease for leakage at valve1

Figure 13 shows the variation in wavelengths of the two FBG sensors in the experiment. The time difference of the two arrived signals is -0.055 s which is closest to the time of valve 2 in Table 4.

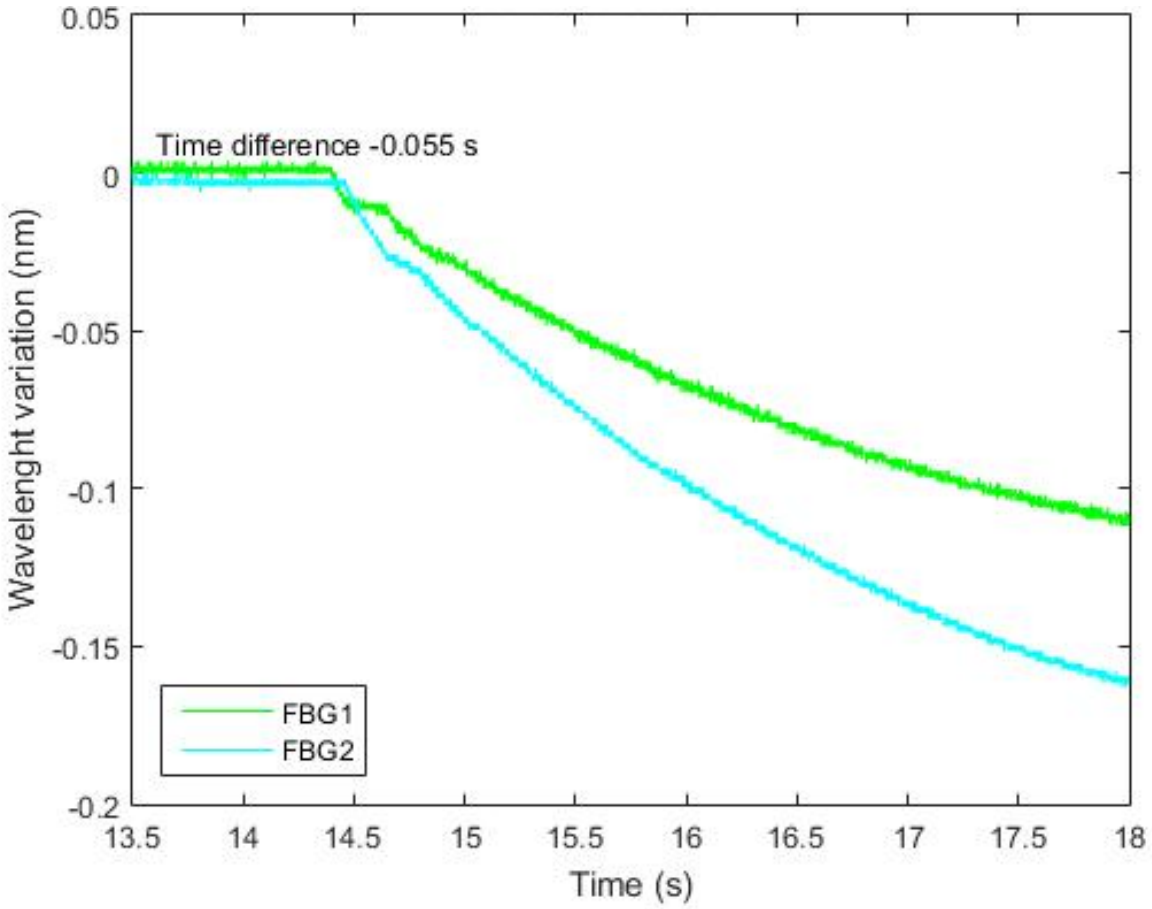

Figure 13-Wavelength decrease for leakage at valve 2

Figure 14 shows the variation in wavelengths of the two FBG sensors in the experiment. The time difference of the two arrived signals is 0.017 s which is closest to the time of valve 3 in Table 3.

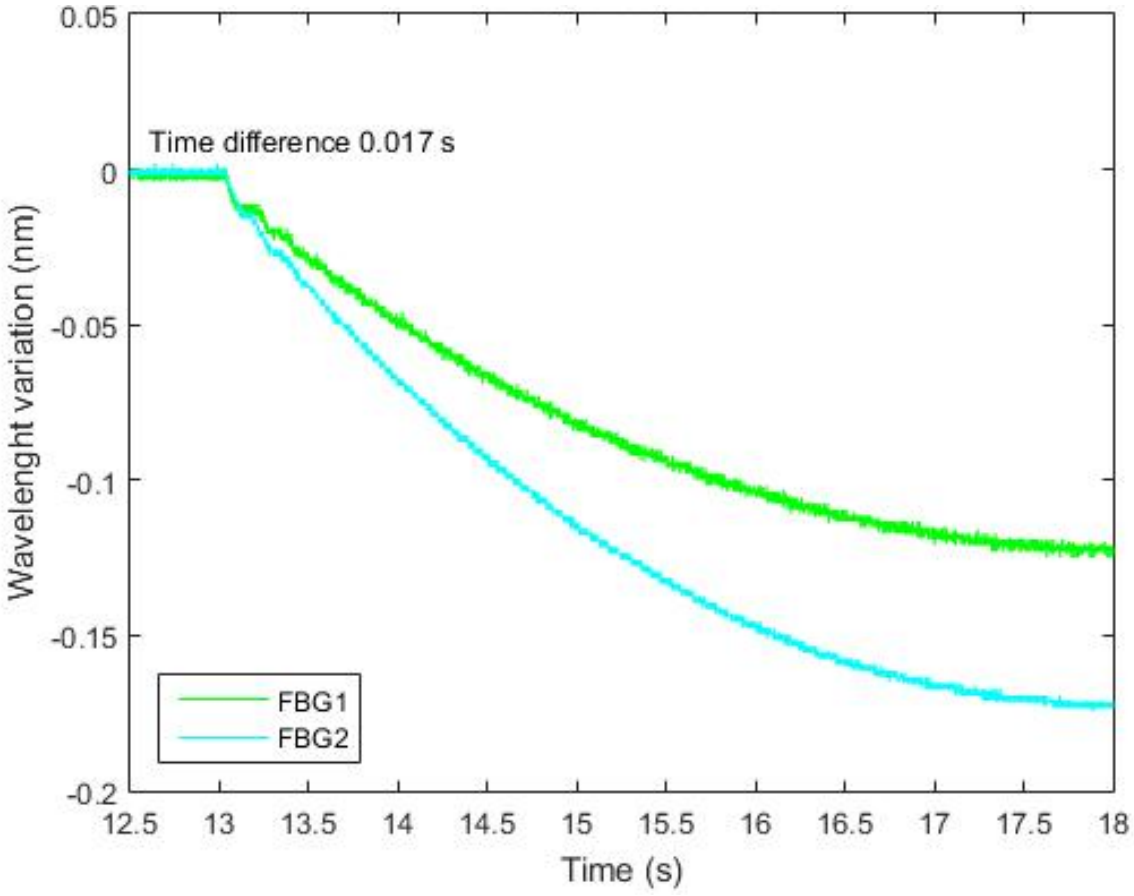

Figure 14-Wavelength decrease for leakage at valve 3

Figure 15 shows the variation in wavelengths of the two FBG sensors in the experiment. The time difference of the two arrived signals is 0.075 s which is closest to the time of valve 4 in Table 3.

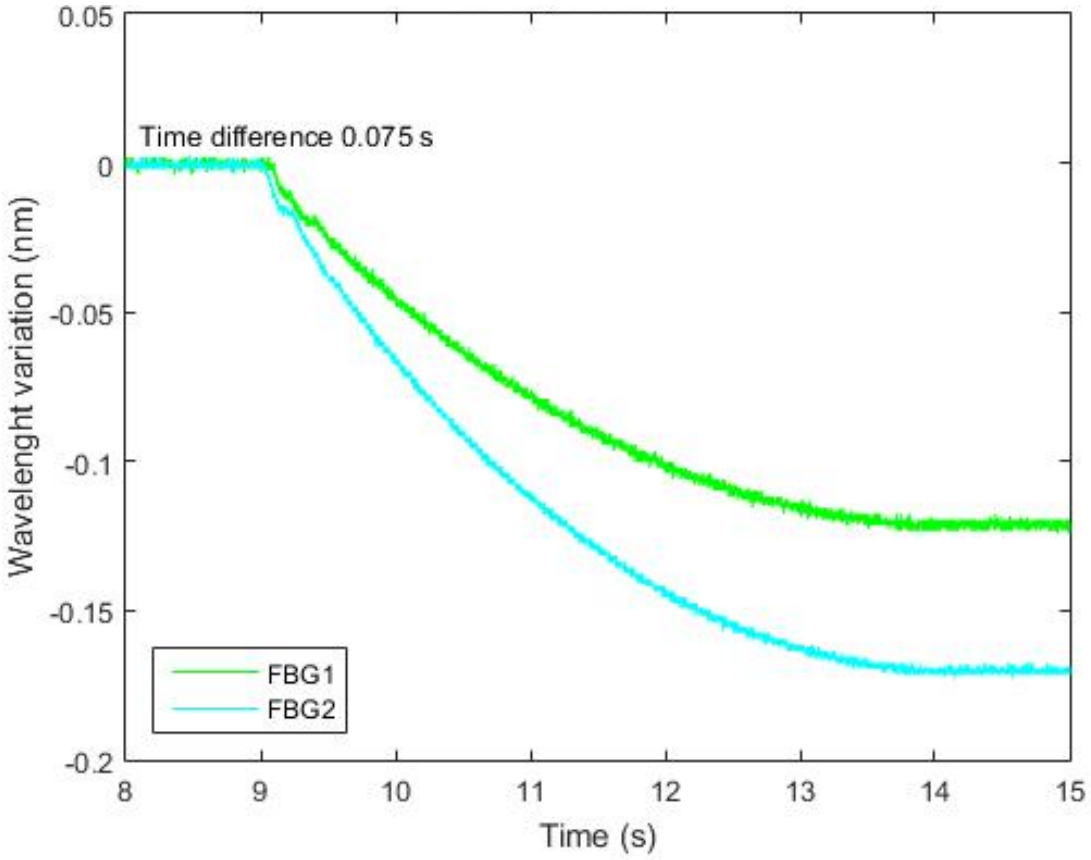

Figure 15-Wavelength decrease for leakage at valve 4

Figure 16 shows the variation in wavelengths of the two FBG sensors in the experiment. The time difference of the two arrived signals is 0.119 s which is closest to the time of valve 5 in Table 3.

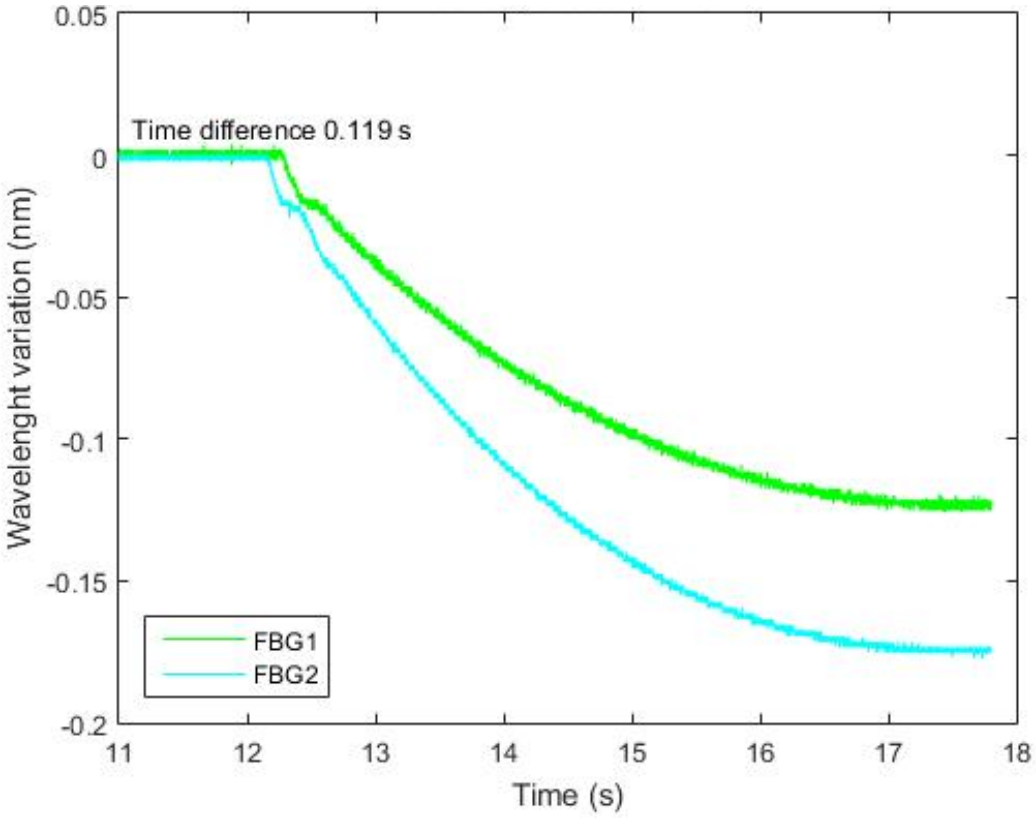

Figure 16-Wavelength decrease for leakage at valve 5

The Real-time LabVIEW interface was designed using Boolean indicators representing each valve. Based on the theory, there is a specific time of arrival difference for each valve on the set-up (ΔT_i). Based on the standard deviation (S) of experiment data, a margin range with the minimum ΔT_i-3S and maximum ΔT_i+3S was defined for each valve (V_i) where any measurement in those range results in correct detection. Considering that, Figure 17 shows the percentage of correct valve detection for 10 experiments done on each valve and total of 50 experiments. However in the real situations, the leakage points could be any location along the pipeline.

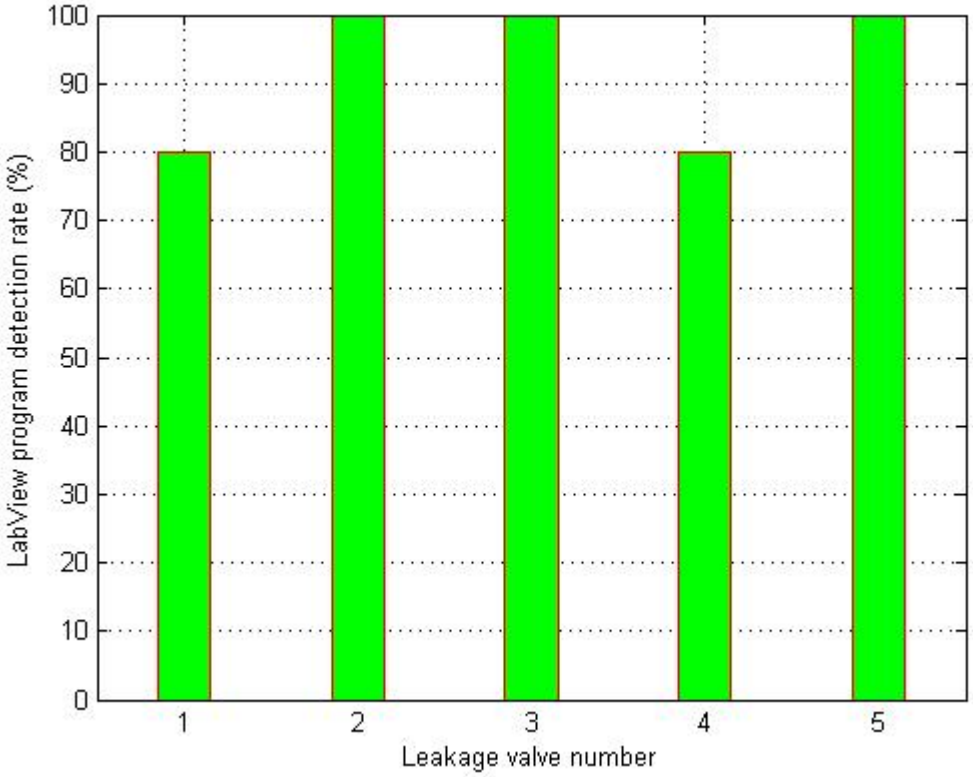

Figure 17-Bar graph showing the amount of correct detections

The rate of accuracy in valves 1 and 4 are less which is because of the reflection of the pressure wave, at the beginning and ending points of the pipeline. A leak in a pipe causes partial reflections of wave fronts that become small pressure discontinuities in the original pressure trace and increase the damping of the overall pressure signal.

The results of the experiment containing all attempts are shown in Figure 18. The actual locations of the valves on the pipeline from the inlet are 31 ft, 54 ft, 82 ft, 111 ft and 135 ft respectively to L_1, L_2, L_3, L_4 and L_5.

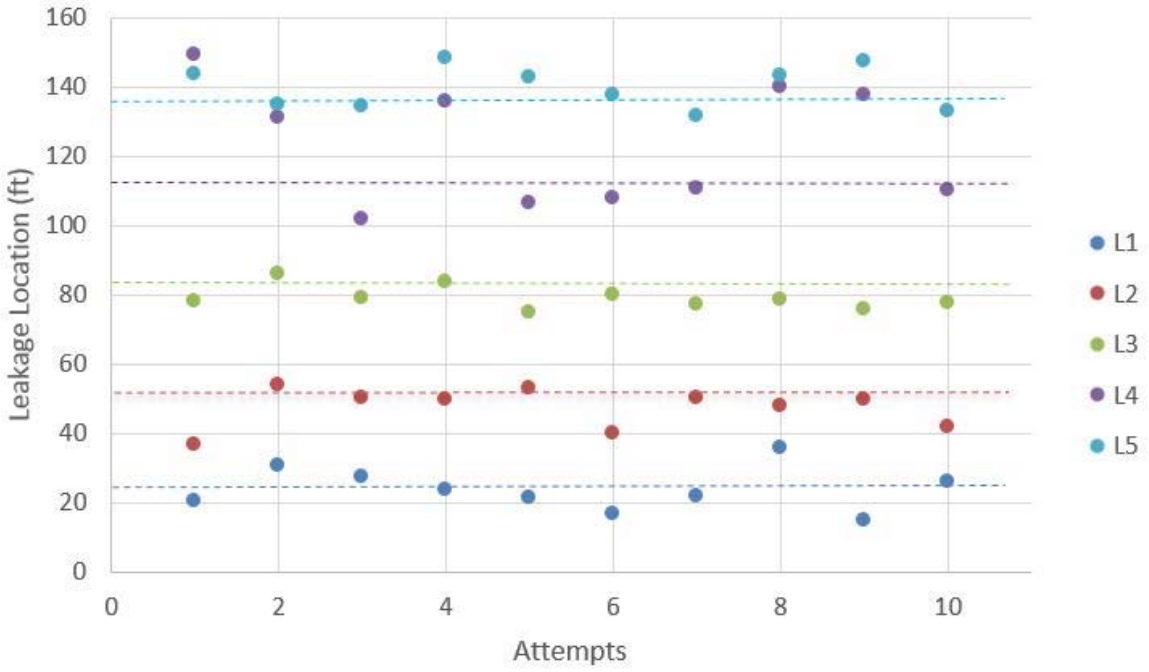

Figure 18-Distribution of the experiment results

Figure 19 shows the standard deviation of the leakage experiments. The blue points show the average of experimental location and the orange points show the actual

location of the leakage. In attempts for valve 4, the results were relatively more than the other values.

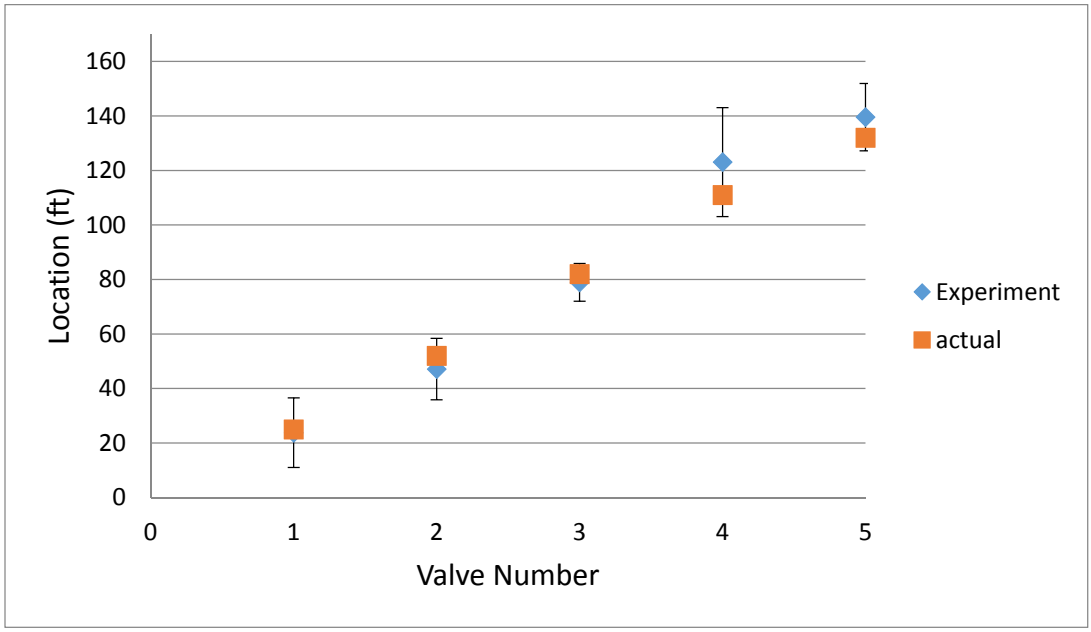

Figure 19-Standard deviation of the experiment results

Table 6 lists the average error of the leakage tests. The highest values for errors are for valves 1 and 5 which is because of the wave propagation reflection:

Table 6- Errors of the leakage experiment

Valve	Error %
1	11
2	6
3	9
4	20
5	11

3. Impact Detection

As shown in the literature, there have been numerous studies about the SHM of pipelines using various sensors to find the leakage location of pipelines. However, there was no experiment in the literature regarding the impact detection of pipelines using FBG sensors. Also, in this thesis, attempts were made to provide the real environment such as travelling to the near-shore areas and performing experiment under seawater. In this experiment two possible hazards that pipelines can have are studied: impact and leakage.

Damage from impacts to pipelines due to third party action is considered the number one cause of pipeline failures [28]. Pipeline operators need to know about pipeline impact events in order to investigate and determine appropriate responses to such events. Current pipeline damage detection methods, such as periodic surveying of pipelines, generally need to be carried out often, or are too costly to provide a truly economical and effective means to safe guard against damage. While many solutions have been developed for leak detection, not much effort has been reported to try providing a self-contained, real time impact detection system that that does not require landline or cell connectivity for communication.

3.1 Literature

Olugboji [28] presented the development and testing of mathematical techniques for locating an impulsive event on a pipeline using the pressure pulse caused by it. From these measurements, the location of the event could be determined and validated the theory by experiments using a model pipeline. Horr and Safi [29] simulated the dynamic responses of a tall building induced by a high speed flying object using complex spectral element method. Hu et al. [30] used an efficient technique to identify impact force acting on CFRP laminated plates using Chebyshev polynomial to approximate the impact force history. Lafayette [31] used a frequency domain deconvolution method to help clarify some of the fundamental difficulties and issues involved to find the force history of the impact. Shrestha et al. [32] proposed 1-dimensional (1D) array fiber Bragg grating (FBG) sensor configuration for impact localization of random impact points on composite wing. Tobias [33] showed a general method of calculating the location of defects in two dimensions based on the difference in time of detection of an emission from the defect at different sensors. Martin et al. [34] demonstrated that the phase information obtained from a spectral analysis of disperse waves can be used to locate the source of the waves. He was able to accurately locate the origin of a dispersing pulse. Shin et al. [35] established an impact monitoring system using fiber Bragg grating (FBG) sensors which had the ability to detect very low to medium energy impacts on an aluminum plate and a long wind turbine blade. By employing two intensity demodulation schemes with different demodulation sensitivities and ranges, he differentiated the relative importance

of the above limiting effects. He also [36] demonstrated that in an impact occuring within ±60 degrees on either sides of the FBG axis, they could measure the location accurately to less than 1 cm. Allison et al. [37] improved the detection accuracy by using FBG rosettes with two mutually perpendicular FBGs. It was shown that with the rosette array, good location accuracy could virtually be extended to all over the plate. They also [37] designed a system for detecting and locating harmful impacts to pipelines using sensors placed along pipelines. They measured the acoustic noise reduction in a pipe section, which propagates at long distances in the pipeline at the specific speed of sound for the particular type of pipe material. Frieden et al. [38] presented a method for the localization of an impact and identification of damage using dynamic strain signals from fiber Bragg grating (FBG) sensors. The data utilized in the method were the arrival times of the asymmetric zero order Lamb waves at the different sensors. A high rate interrogation method based on intensity modulation of the Bragg wavelength shift is used to acquire the FBG signals. Gomez et al. [39] proved that optical fibers with Bragg gratings can be used to detect impacts, and also that a high-frequency interrogator is necessary to collect valuable information about the impacts. Betz et al. [40] tested a damage detection and damage localization system based on fiber Bragg grating sensors. Their damage identification system involved Bragg gratings for sensing ultrasound by detecting the linear strain component produced by Lamb waves. Making use of the directional properties of the Bragg grating the direction of the reflected acoustic waves were determined by mounting three of the gratings in a rosette configuration. Chan et al.

[41] investigated the feasibility of using the developed FBG sensors for structural health monitoring, via monitoring the strain of different parts of a bridge in Hong Kong under both the railway and highway loads as well as comparing the FBG sensors' performance with the conventional structural health monitoring system.

3.2. Methodology

The methodology for impact detection is quite similar to the leakage detection that was earlier explained in section 2.2. An impulsive event occurring along a pipeline generates surface wave which propagate in both directions and this can be detected and measured by sensors located at different positions along the pipeline. By finding the time difference of the received signals and based on the velocity of the wave propagation speed (2380 m/s), the impact location can be estimated using eqn. (7).

3.3. Experimental Setup

The present experiment relates to pipelines, and more particularly, to a system for improving pipeline safety by detecting and locating third party impacts to a pipeline that may cause damage to the pipeline and informing operators about the third party impacts in real-time. In the following sections, information about the set up of the pipeline and sensors orientation are provided.

3.3.1 Lab Model

The set up for the impact detection experiment was the same as leakage detection experiment. Twelve new sensors were bonded and installed on the pipe unlike

the leakage experiment where only two sensors were used. FBGs were installed along the axis of the pipe in order to mechanically filter out hoop strain. The mechanism behind the filter is that impact events will cause axial and lateral strains but minimal hoop strain. On the other hand, leakage events are characterized by hoop strain with minimal axial and lateral strains. Figure 20 shows the schematic of the pipeline with the location of the sensors on each row.

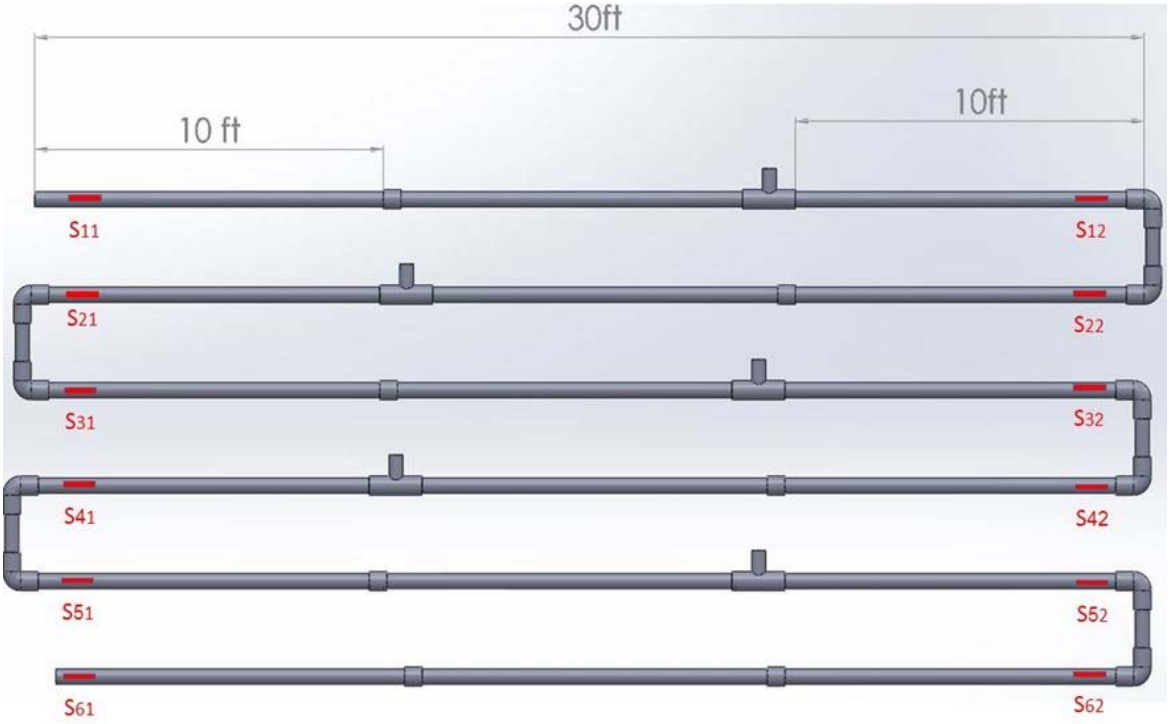

Figure 20-The layout of the pipeline for the experiment with the sensors location

Each sensor for the impact experiment was installed on the axial direction because the vibrations induced by the impact have no components acting on other directions. Figure 21 and Figure 22 show the orientation of the sensors on the pipes.

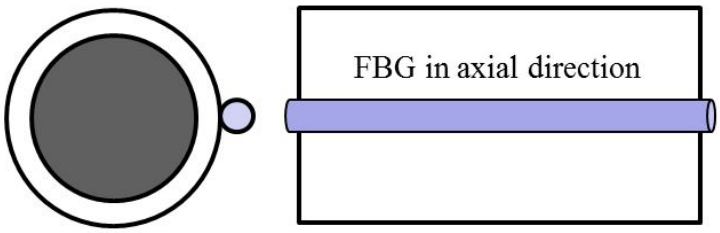

Figure 21-Schematic orientation of the sensor on the pipeline

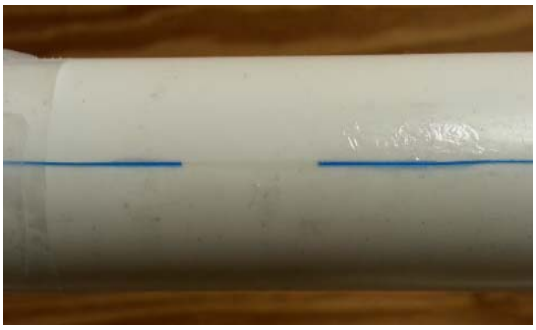

Figure 22-The orientation of sensor

3.3.2. Programming Algorithm

The program code was developed in LabVIEW. It consists of block diagrams that create a graphical interface for the user to observe the data of each sensor connected through the interrogator. Algorithm of the LabVIEW code is presented in Figure 23 and described in steps below:

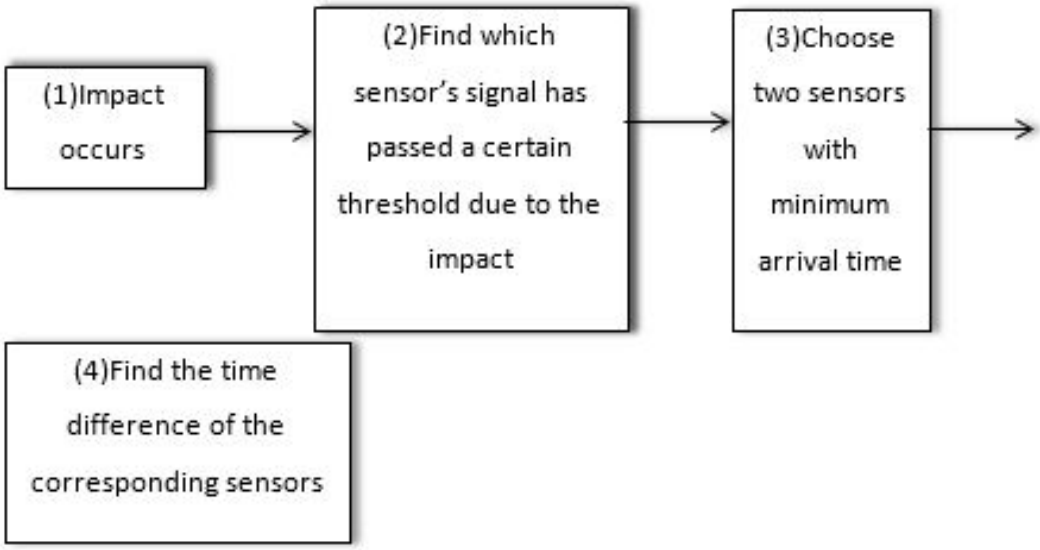

Figure 23-Algorithmic flowchart of the code

1. Impact: when the impact occurs, there is an impulse in the wavelength of the sensors and significant increase in the signal amplitude. Therefore by defining a threshold and using a threshold detector on the program, one is able to detect if the impact has occurred or not.
2. All sensors receive the signal as long as they work properly and if the impact energy is not attenuated during propagation. It is evident that the two sensors closest to the impact location at each side have the smallest magnitude of the time of arrival.
3. The algorithm stores all the time of arrival data in an array and then sorts them all in magnitude increasing order. Then the first two elements are extracted.
4. Now that the sensors locations are already known. Using eqn. (7), the exact location of the impact is found.

3.3.3. Experimental Results

A total number of twelve FBGs were installed on all six rows of the pipeline. Every four sensors were connected to one channel of the interrogator. They are all listed in Table 7:

Table 7- Wavelength values of the sensors used for the lab experiment

Row #	Wavelengths of FBGS (nm)		Channel #
1	1520	1559	2
2	1530	1535	
3	1545	1550	3
4	1555	1575	
5	1550	1570	4
6	1580	1585	

It was considered not to use two sensors with the same wavelength in the same channel. Every four sensors were connected sequentially to one channel of the interrogator. Channel 1 was designated for the leakage test in case both tests are done simultaneously. Figure 24 shows the locations were the impact was tested on the pipeline with green arrow.

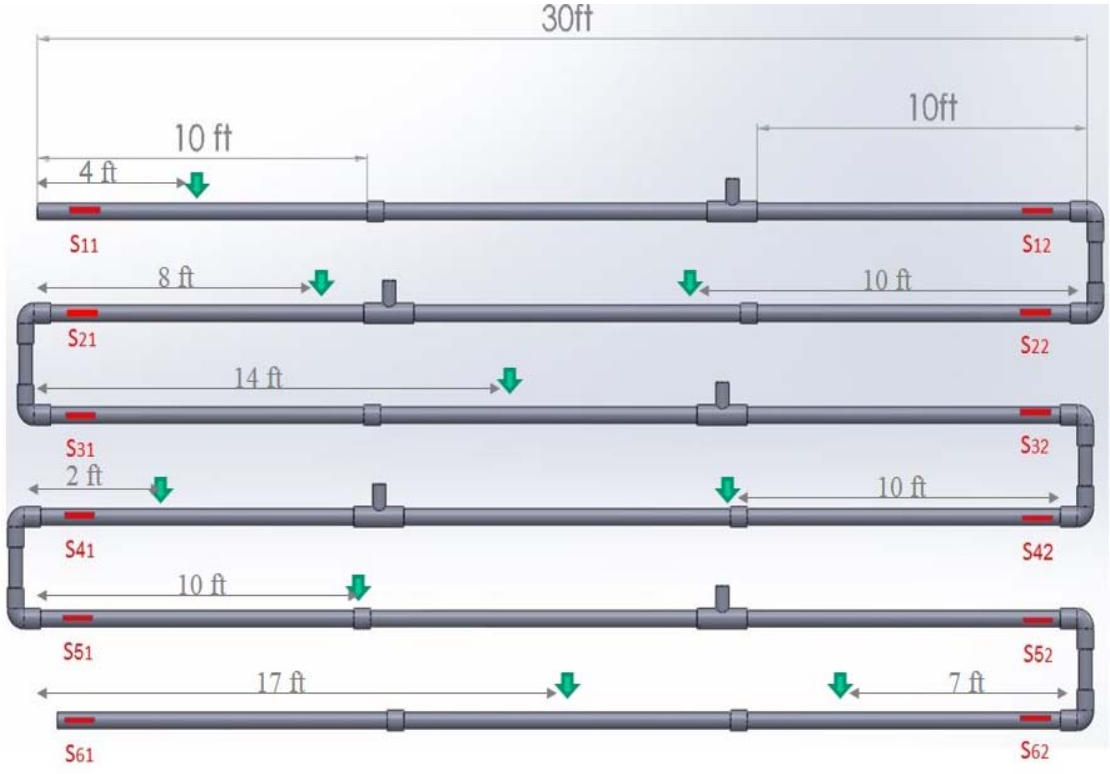

Figure 24- Locations were impact was tested

Table 8 contains the data of impact the experiment, where the location numbers were defined on various points of the pipeline, the average of ten experiments was conducted at each indicated points. The actual location on this table is in fact the relative location to the inlet of the corresponding row.

Table 8- Data of the impact detection experiment

Location #	Average Time difference (s)	Actual Location (ft) relative to the inlet	Calculated Location (ft)	Relative error %	Standard deviation
1	-0.0887	1.54	2.85	15.00	0.0168
2	-0.0820	4.21	3.50	35.00	0.0251
3	-0.0750	5.88	4.22	16.32	0.01109
4	-0.0476	8.21	7.09	10.46	0.1086
5	-0.0149	10.08	10.40	9.80	0.0119
6	-0.0276	12.04	11.80	8.60	0.0168
7	0.0182	14.13	13.80	4.20	0.0072
8	0.0377	16.13	15.80	5.80	0.0110
9	0.0484	18.33	16.90	9.02	0.0110
10	0.0770	20.00	19.90	10.80	0.0239
11	0.0670	22.20	18.90	15.80	0.0110

Figure 25 shows the error of the results. The closer the impact location to the sensor, the higher error is observed. The reason could be the low sampling rate of the data acquisition device which makes the minimum resolution of 2.3 meters distance from each sensor to acquire data and the variation of the experiments data are presented in Figure 26.

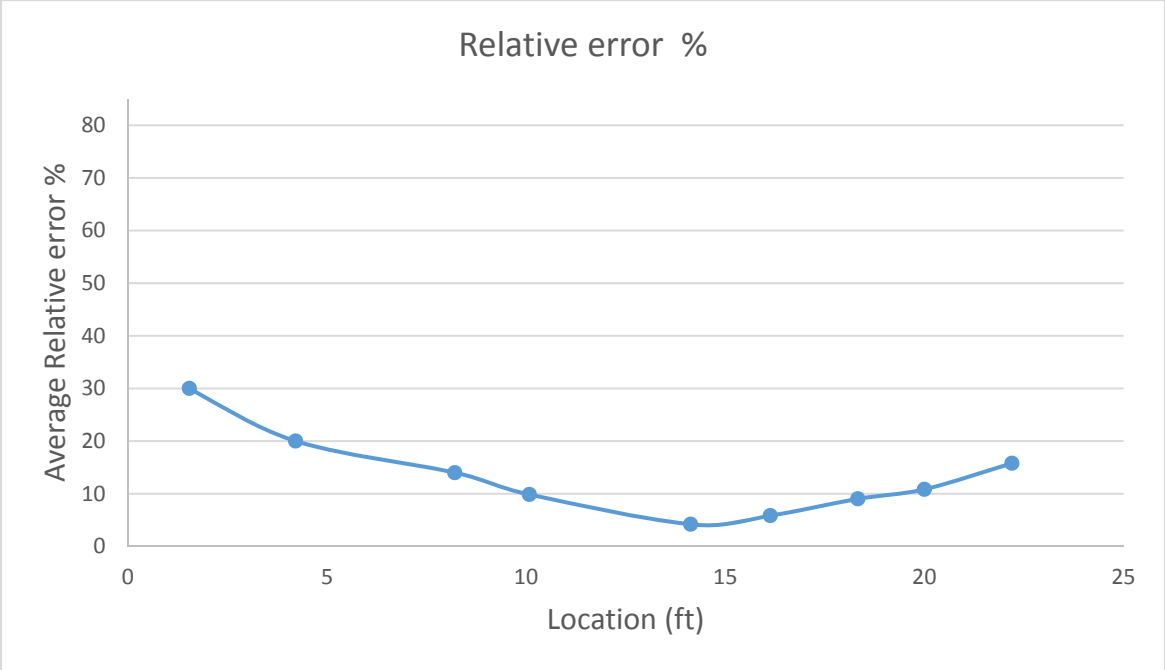

Figure 25-Relative error of the impact detection test

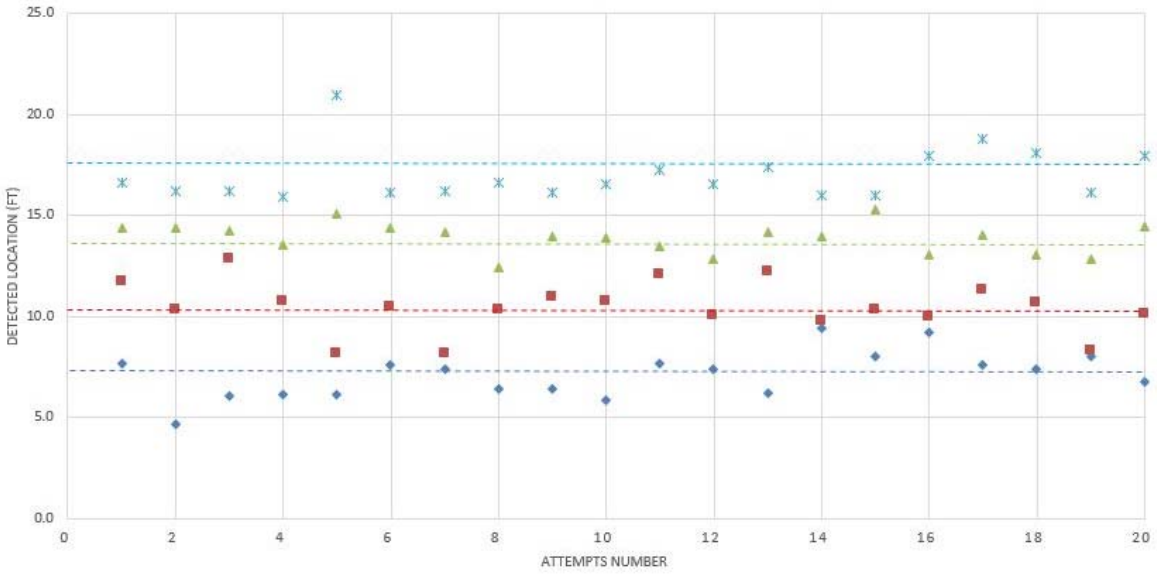

Figure 26-The variation of the experiment data

3.4. Impact Test on a Submerged Pipeline Model

To demonstrate the reliability of the method in detecting conditions of subsea pipelines, similar experiment of impact detection experiment under was carried out on a submerged pipeline model. Subsea pipelines lie on the seabed and are submerged under water hundreds of mile below sea level.

The difficulty of access to the pipelines, makes their structural health monitoring more challenging. In order to obtain results that are closer to real conditions, the experiment was conducted in Galveston beach in Texas, US. Table 9 lists the parameters of the pipeline.

Table 9-Submerged pipeline experiment data

Date	Sep 19 2015
Location	Sunny beach, Galveston, TX,USA
Longitude	-94.9
Latitude	29.2
Total length	41 ft
Horizontal Rows length	20 ft
Vertical Rows length	1 ft
Number of sensors	6

3.4.1. Experimental Setup

Figure 27 shows the assembled pipeline laying on the shore before conducting the experiment. The pipeline components were assembled at the experiment location, otherwise the delivery from the university lab to the experiment site would be costly and time-consuming. The yellow cables are fiber optic cables that connect the FBG sensors. In order to constrain the cables to the pipelines, electric tapes were used.

Figure 27-The assembled pipeline ready for the experiment

Figure 28 shows the whole setup of the experiment. There were total 6 poles in the sea to stabilize the pipe against sea waves. In order to avoid the possible hazard of swimmers not seeing the pipeline, pink balloons were tied to the pipeline to make it distinct.

Figure 28-The pipeline connected to the poles in the water during the experiment

In order to facilitate the assembly and disassembly, the pipe was prepared in parts of 5 ft and then connected through connectors for assembly. Figure 29 shows the schematic drawing of the pipeline and the sensors locations on it.

Figure 29-Schematic layout of the pipeline for the submerged experiment

3.4.2. Experimental Results

There were six sensors bonded on the pipeline for the submerged experiment. Three sensors at each row installed at the beginning, middle and end of each row. Sensors at each row were connected together on a single span of fiber and were connected to two channels of the interrogator. However, four were damaged during transportation from the lab to the beach. With the remaining two sensors, 30 experiments were done at three different points of the pipeline. The real-time code was not able to find the location correctly because of the effect of the sea water motion. In Table 10, the time arrival differences for all 30 attempts are shown and Figure 30 shows the locations of the impact test.

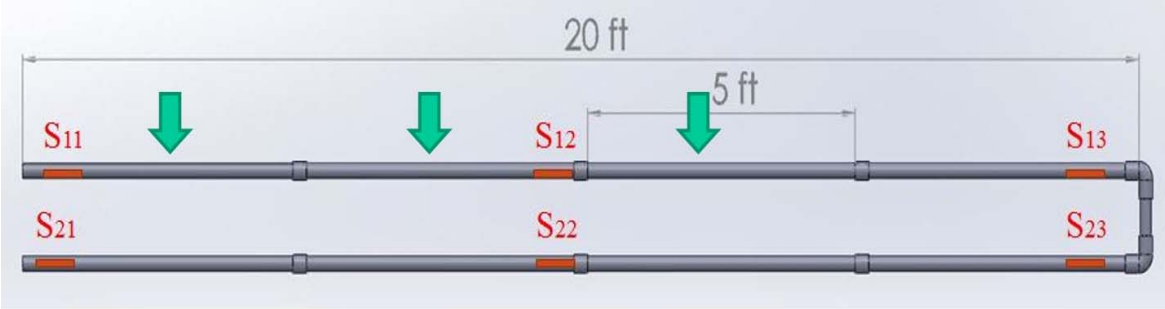

Figure 30- Locations of the impact test

Table 10- Results of the impact detection experiments at the submerged model

Attempt	Time difference (s) Point 1	Time difference (s) Point 2	Time difference (s) Point 3
1	-0.002	0.014	-0.014
2	-0.002	0.009	-0.021
3	-0.002	-0.003	-0.011
4	-0.003	0.007	-0.014
5	-0.001	0.006	-5.771
6	-0.004	0.009	-0.016
7	-0.002	0.011	-0.014
8	-0.002	0.013	-0.017
9	-0.004	0.011	-0.012
10	-0.002	0.009	-0.011

Figure 31 and Figure 32 show the recorded signal of two sensors during the impact. As it is seen in these figures, the impact signal is obvious and is similar to an impulse function. However, in Figure 32, the effect of sea current motion is clearer. Since the impact location is closer to the first sensor, the amplitude of the impulse almost twice as high.

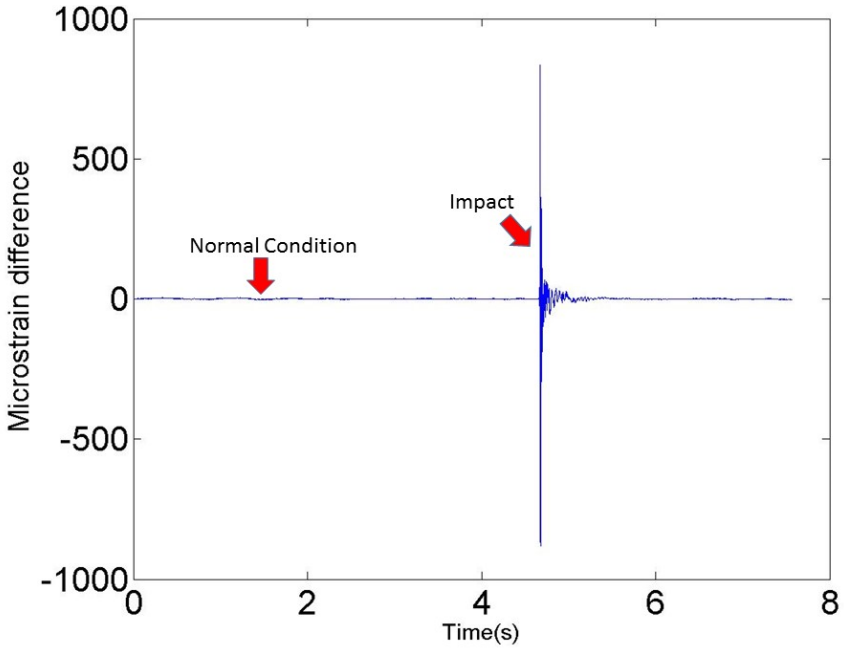

Figure 31-Sensor 1 unfiltered signal

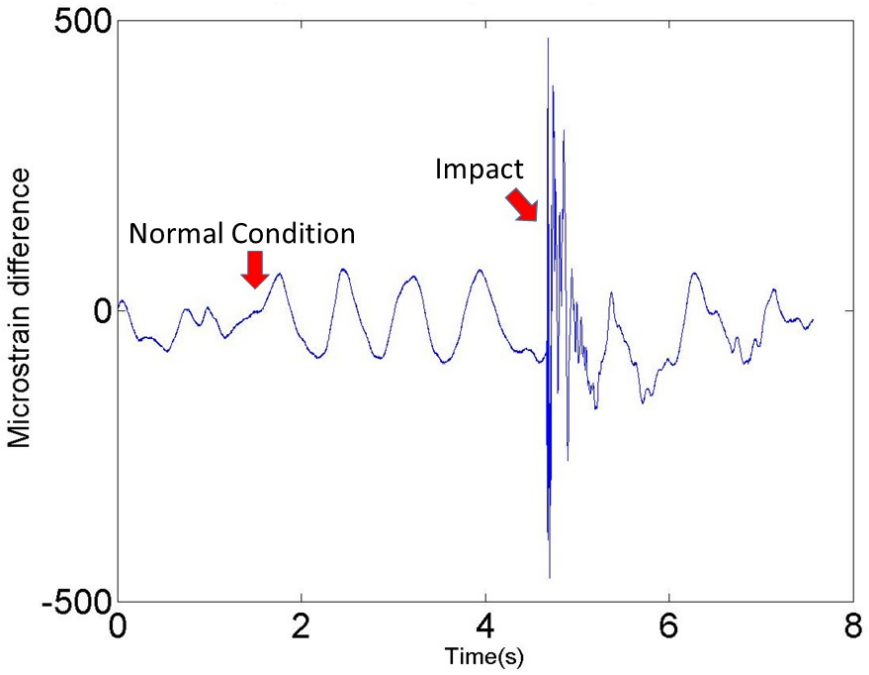

Figure 32-Sensor 2 unfiltered signal

The oscillation of the signal is due to the sea current and it shows that the FBG sensor can be used in the subsea pipelines. However in order to able to process the data more effectively, we can cancel out the effect of sea wave using high-pass filters as we know that the sea waves frequencies are relatively small. Therefore, a Butterworth high-pass filter is added using MATLAB "fdatool" and implemented on the code.

Power spectral density function (PSD) shows the strength of the variations (energy) as a function of frequency. In other words, it shows at which frequencies variations are strong and at which frequencies variations are weak. The unit of PSD is energy per frequency (width) and the energy can be obtained within a specific frequency range by integrating PSD within that frequency range. Computation of PSD is done directly by the method called FFT or computing autocorrelation function and then transforming it. The PSD analysis is done by MATLAB and eqn. (10) is the formula for Butterworth filter in the frequency domain

$$\left| H(j\omega) = \frac{1}{1+\left(\frac{\omega}{\omega_c}\right)^2} \right|. \tag{10}$$

The designed high-pass Butterworth filter had a cut-off frequency of ω_c= 50 Hz and order of n=3 and $|H(j\omega)|$ is the amplitude of the signal in frequency domain. Once the filter is applied to the data, the signal is clean without any noticeable effects of the sea current on the sensor signals.

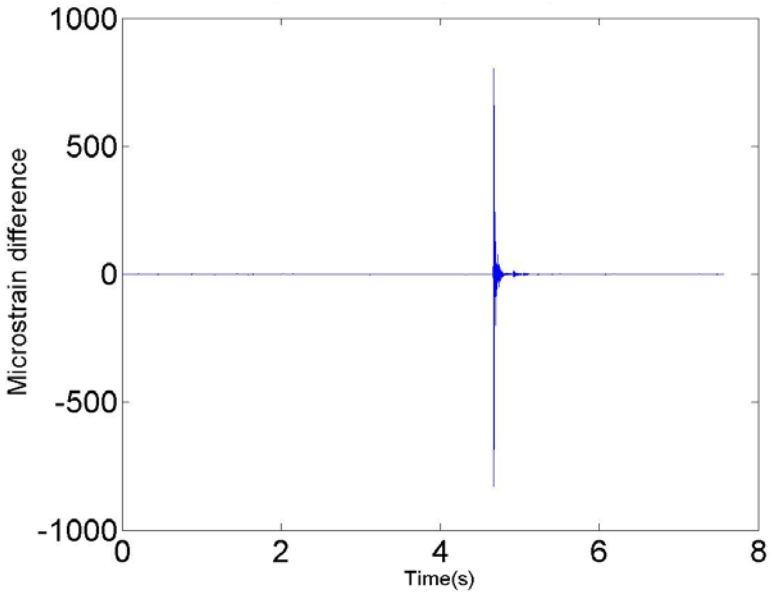

Figure 33-Sensor 1 filtered signal

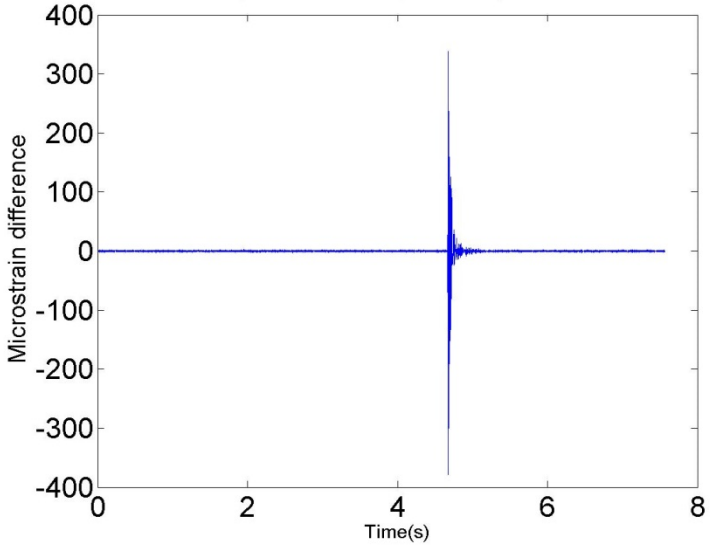

Figure 34-Sensor 2 filtered signal

As seen in Figure 33 and Figure 34, the high-pass filter has cancelled the effect of the sea motion and with this modification, the values of the time difference can be found

easily by using cross-correlation method. The average of the total impact experiments for the submerged model is in Table 11.

Table 11- Relative error of the experiments of submerged pipeline

Location #	Actual distance(ft)	Calculated distance(ft)	Relative Error(%)
1	2.5	3.25	30
2	7.5	9.075	21
3	12	16.2	36

The other reason for observing noticeable error in the results is the small distance of the sensor from the impact location. With the 1 kHz sampling frequency of the interrogator, the smallest detectable time for the device would be 0.001 s and with the propagation speed of 2380 m/s in PVC pipeline, the impact location should have at least 2.3 m distance from each sensor.

4. Conclusions

This thesis presents a novel method for the real-time detection of impact and leakage in subsea pipelines. First, a model pipeline using PVC was installed in the lab to conduct the experiments. The first set of experiments were conducted for the leakage tests, in which the leakage events were created by opening one of the five ball valves. Using the principle of NPW, the real-time LabVIEW program was able to detect the right location of the leakage with high accuracy. The second part of the thesis was detection and localization of impact using the same theory. Furthermore, once the feasibility of NPW theory and using FBG sensors were tested in the lab, the same experiment was conducted in sea shore while the pipeline was exposed to sea water and real conditions of operating subsea pipelines.

The experiments demonstrated that FBG sensors are great options for structural health monitoring of subsea pipelines. However, two main challenges were observed during this experiment: (1) Noise is generated by the equipment and also the background wooden wall which the pipeline relies on. (2) The pressure wave attenuates due to energy dissipation as it propagates along the pipeline. The attenuation increases with pipe bends, constrictions in the pipeline, and two-phase conditions. Therefore, small leak detection approaches should have the ability to recognize weak signals with obscure leak features, and locate them accurately.

(3) The wave propagation speed is relatively higher in the impact test than the leakage test. As a result, the required sampling rate for the impact test should be more for the impact test as the speed of propagation is 2380 m/s in the impact event.

References

1. Lopez-Higuera, J.M., L. Rodriguez Cobo, A. Quintela Incera, and A. Cobo, "Fiber Optic Sensors in Structural Health Monitoring." *Journal of Lightwave Technology*, 2011. **29**: p. 587-608.
2. Li, H.N., D.S. Li, and G.B. Song, "Recent applications of fiber optic sensors to health monitoring in civil engineering." *Engineering Structures*, 2004. **26**: p. 1647-1657.
3. Daniele Inaudi, B.G., "Long-Range Pipeline Monitoring by Distributed Fiber Optic Sensing." *Pressure Vessel Technology*, 2010. **132**.
4. Vanniamparambil, P.A., I. Bartoli, K. Hazeli, J. Cuadra, E. Schwartz, R. Saralaya, and A. Kontsos, "An integrated structural health monitoring approach for crack growth monitoring." *Journal of Intelligent Material Systems and Structures*, 2012. **23**: p. 1563-1573.
5. Majumder, M., T.K. Gangopadhyay, A.K. Chakraborty, K. Dasgupta, and D.K. Bhattacharya, "Fibre Bragg gratings in structural health monitoring—Present status and applications." *Sensors and Actuators A: Physical*, 2008. **147**: p. 150-164.
6. Pinet, E., C. Hamel, B. Gliic, D. Inaudi, and N. Miron, "Health monitoring with optical fiber sensors: From human body to civil structures." *Health Monitoring of Structural and Biological Systems 2007, March 19, 2007 - March 22, 2007*, 2007. **6532**: p. SPIE; American Society of Mechanical Engineers, AS.
7. Urban, F., J. Kadlec, R. Vlach, and R. Kuchta, "Design of a pressure sensor based on optical fiber Bragg grating lateral deformation." *Sensors*, 2010. **10**: p. 11212-11225.

8. Sohn, H., K. Worden, and C.R. Farrar, "Statistical Damage Classification Under Changing Environmental and Operational Conditions." *Journal of Intelligent Material Systems and Structures*, 2002. **13**: p. 561-574.

9. Werneck, M.M., R.C.S.B. Allil, B.A. Ribeiro, and F.V.B.D. Nazaré, "A Guide to Fiber Bragg Grating Sensors." 2013: p. 1-24.

10. Doyle, C., "Fibre Bragg Grating Sensors-An Introduction to Bragg gratings and interrogation techniques." *Smart Fibres Ltd*, 2003: p. 1-5.

11. Kim, S.H., "Extensive Development of Leak Detection Algorithm by Impulse Response Method." *Hydraulic Engineering*, 2005. **131**(3): p. 201-208.

12. Hou, Q., J. Wenling, Z. Shuhui, R. Liang, and J. Ziguang, "Natural Gas Pipeline Leakage Detection Based on FBG Strain Sensor." *2013 Fifth International Conference on Measuring Technology and Mechatronics Automation*, 2013: p. 712-715.

13. Huang, J., Z. Zhou, D. Zhang, and Q. Wei, "A fiber bragg grating pressure sensor and its application to pipeline leakage detection." *Advances in Mechanical Engineering*, 2013. **2013**.

14. Ma, C., S. Yu, and J. Huo, "Negative pressure wave-flow testing gas pipeline leak based on wavelet transform." *2010 International Conference on Computer, Mechatronics, Control and Electronic Engineering, CMCE 2010*, 2010. **5**: p. 306-308.

15. Mandal, S.K., F.T.S. Chan, and M.K. Tiwari, "Leak detection of pipeline: An integrated approach of rough set theory and artificial bee colony trained SVM." *Expert Systems with Applications*, 2012. **39**: p. 3071-3080.

16. Da Silva, H.V., C.K. Morooka, I.R. Guilherme, T.C. da Fonseca, and J.R.P. Mendes, "Leak detection in petroleum pipelines using a fuzzy system." *Journal of Petroleum Science and Engineering*, 2005. **49**: p. 223-238.

17. Qiong, H. and F. Shidong, "Development of Pipeline Leak Detection System based on LabVIEW." *2008 IEEE International Symposium on Knowledge Acquisition and Modeling Workshop*, 2008: p. 671-674.

18. Laurentys, C.A., C.H.M. Bomfim, B.R. Menezes, and W.M. Caminhas, "Design of a pipeline leakage detection using expert system: A novel approach." *Applied Soft Computing*, 2011. **11**: p. 1057-1066.

19. Lu, X., Y. Sang, J. Zhang, and Y. Fan, "A Pipeline Leakage Detection Technology based on Wavelet Transform Theory." *2006 IEEE International Conference on Information Acquisition*, 2006: p. 1432-1437.

20. Hou, Q., L. Ren, W. Jiao, P. Zou, and G. Song, "An improved negative pressure wave method for natural gas pipeline leak location using FBG based strain sensor and wavelet transform." *Mathematical Problems in Engineering*, 2013. **2013**.

21. Verde, C., "Accommodation of multi-leak location in a pipeline." *Control Engineering Practice*, 2005. **13**: p. 1071-1078.

22. Lee, P.J., J.P. Vítkovský, M.F. Lambert, A.R. Simpson, and J.A. Liggett, "Leak location using the pattern of the frequency response diagram in pipelines: A numerical study." *Journal of Sound and Vibration*, 2005. **284**: p. 1051-1073.

23. Lopes dos Santos, P., T.P. Azevedo-Perdicoúlis, G. Jank, J.A. Ramos, and J.L. Martins de Carvalho, "Leakage detection and location in gas pipelines through an LPV identification

approach." *Communications in Nonlinear Science and Numerical Simulation*, 2011. **16**: p. 4657-4665.

24. Zhu J., S.C.H., Ziguang J., Song G. "Gas pipeline Leakage Detection Based on PZT Sensors," in *CANSMART*. 2015: Vancouver, Canada.

25. Ge, C., G. Wang, and H. Ye, "Analysis of the smallest detectable leakage flow rate of negative pressure wave-based leak detection systems for liquid pipelines." *Computers and Chemical Engineering*, 2008. **32**: p. 1669-1680.

26. Ren, L., Z.G. Jia, H.N. Li, and G. Song, "Design and experimental study on FBG hoop-strain sensor in pipeline monitoring." *Optical Fiber Technology*, 2014. **20**: p. 15-23.

27. Optics, M., "Dynamic Optical Sensing Interrogator ," M. Optics, Editor. 2015.

28. Olugboji, O.A., "Development of an impact monitoring system for petroleum pipelines." *Methods*, 1998. **15**: p. 115-120.

29. Horr, A.M. and M. Safi, "Impact wave propagation in tall buildings using advanced spectral element method." *Structural Design of Tall and Special Buildings*, 2003. **12**: p. 127-143.

30. Hu, N., H. Fukunaga, S. Matsumoto, B. Yan, and X.H. Peng, "An efficient approach for identifying impact force using embedded piezoelectric sensors." *International Journal of Impact Engineering*, 2007. **34**: p. 1258-1271.

31. Lafayette, W., "Impact Force Identification from Wave propogation Responses." *Science*, 1996. **18**.

32. Shrestha, P., J.H. Kim, Y. Park, and C.G. Kim, "Impact localization on composite wing using 1D array FBG sensor and RMS/correlation based reference database algorithm." *Composite Structures*, 2015. **125**: p. 159-169.

33. Tobias, A., "Acoustic-emission source location in two dimensions by an array of three sensors." *Non-Destructive Testing*, 1976. **9**: p. 9-12.

34. Martin, M.T. and J.F. Doyle, "Impact force location in frame structures." *International Journal of Impact Engineering*, 1996. **18**: p. 79-97.

35. Shin, C.S., B.L. Chen, and S.K. Liaw, "An FBG-based impact event detection system for structural health monitoring." *Advances in Civil Engineering*, 2010. **2010**.

36. Shin, C.S. and B.L. Chen, "An impact source locating system using fiber Bragg grating rosette array." *3rd International Conference on Smart Materials and Nanotechnology in Engineering*, 2012. **8409**: p. 1-6.

37. Peter S. Allison, C.E.C., Bryan Lethcoe, "Acoustic Impact Detection and Monitoring System.".2009, General Electric Company, Schenectady.

38. Frieden, J., J. Cugnoni, J. Botsis, and T. Gmür, "Low energy impact damage monitoring of composites using dynamic strain signals from FBG sensors - Part I: Impact detection and localization." *Composite Structures*, 2012. **94**: p. 438-445.

39. Gomez, J., I. Jorge, G. Durana, J. Arrue, J. Zubia, G. Aranguren, A. Montero, and I. López, "Proof of concept of impact detection in composites using fiber bragg grating arrays." *Sensors (Basel, Switzerland)*, 2013. **13**: p. 11998-12011.

40. Betz, D., G.J. Thursby, B. Culshaw, and W. Staszewski, "Structural damage location with fiber bragg grating rosettes and lamb waves." 2007. **6**: p. 299-308.

41. Chan, T.H.T., L. Yu, H.Y. Tam, Y.Q. Ni, S.Y. Liu, W.H. Chung, and L.K. Cheng, "Fiber Bragg grating sensors for structural health monitoring of Tsing Ma bridge: Background and experimental observation." *Engineering Structures*, 2006. **28**: p. 648-659.

Appendix I

- Leakage/Impact location Formula Derivation

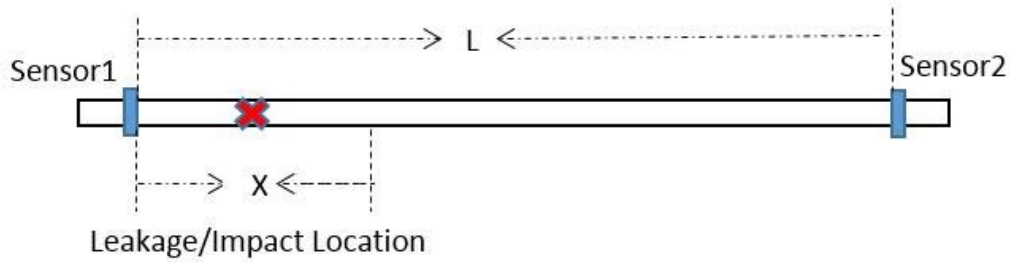

Figure 35-Leakage location formula derivation

In Figure 35, assuming t_1 as the time when the impact or leakage event reaches sensor 1, t_2 as the time it reaches sensor2 and considering the constant velocity of the wave propagation, eqn. (8.1-8.4) represent the governing equations of this event [20]:

$$t_1=\frac{x}{v-u}, \tag{8.1}$$

$$t_2=\frac{L-x}{v+u}, \tag{8.2}$$

$$\Delta t=t_1-t_2 \text{ and} \tag{8.3}$$

$$x=\frac{1}{2v}[L(v-u)+\Delta t(v^2-u^2)], \tag{8.4}$$

where v denotes the wave propagation velocity and u is the inside fluid velocity. Assuming an empty pipeline Eq. 8.4 is simplified to eqn. (9)

$$x=\frac{v\Delta t+d}{2}. \tag{9}$$